Extracellular vesicles are independent metabolic units with asparaginase activity

Nunzio Iraci[1,10,11] , Edoardo Gaude[2,11], Tommaso Leonardi[1,3], Ana S H Costa[2], Chiara Cossetti[1], Luca Peruzzotti-Jametti[1] , Joshua D Bernstock[1,4] , Harpreet K Saini[3], Maurizio Gelati[5,6], Angelo Luigi Vescovi[6,7], Carlos Bastos[8], Nuno Faria[8], Luigi G Occhipinti[9], Anton J Enright[3], Christian Frezza[2]* & Stefano Pluchino[1]*

Extracellular vesicles (EVs) are membrane particles involved in the exchange of a broad range of bioactive molecules between cells and the microenvironment. Although it has been shown that cells can traffic metabolic enzymes via EVs, much remains to be elucidated with regard to their intrinsic metabolic activity. Accordingly, herein we assessed the ability of neural stem/progenitor cell (NSC)-derived EVs to consume and produce metabolites. Our metabolomics and functional analyses both revealed that EVs harbor L-asparaginase activity, catalyzed by the enzyme asparaginase-like protein 1 (Asrgl1). Critically, we show that Asrgl1 activity is selective for asparagine and is devoid of glutaminase activity. We found that mouse and human NSC EVs traffic Asrgl1. Our results demonstrate, for the first time, that NSC EVs function as independent metabolic units that are able to modify the concentrations of critical nutrients, with the potential to affect the physiology of their microenvironment.

EVs are a heterogeneous group of membrane particles secreted by the majority of cell types across all kingdoms of life that have different mechanisms of biogenesis, structural composition and functions[1]. Of these, shedding vesicles, exosomes and apoptotic bodies have been the most studied subtypes of EVs to date[2]. Several studies aimed at characterizing the content of EVs went on to demonstrate that a broad range of bioactive molecules, including proteins and different types of nucleic acids, are associated with EVs[3,4]. Of note, the content of EVs can vary according to the cell type of origin and/or in response to stimuli from the microenvironment[5]. We previously demonstrated that NSCs secrete EVs containing mRNAs and proteins, whose sorting is regulated by inflammatory cytokines. Our study identified a novel mechanism of intercellular communication regulated by the IFN-γ–Ifngr1 (IFN-γ receptor 1) complex on EVs and elucidated its molecular signature and its functional relevance to target cells[6].

A growing body of evidence supports a key a role for EVs in regulating metabolic homeostasis or associated cellular processes. For instance, glucose deprivation was shown to promote trafficking of glucose transporters and glycolytic enzymes toward EVs in cardiomyocytes[7]. Prostate-derived, exosome-like prostasomes harbor enzymes involved in ATP metabolic turnover, which include adenylate kinase, ATPase, 5′-nucleotidase, and hexose transporters[8]. One quarter of the proteins enriched in prostate-cancer-derived EVs large oncosomes (compared to prostate cancer cells) include enzymes involved in glucose, glutamine and amino acid metabolism[9]. Furthermore, primary B-cell precursor acute lymphoblastic leukemia cells release a variety of EVs into extracellular fluids (in vitro) and circulation (in vivo) that are internalized by stromal cells, which subsequently undergo a metabolic switch toward a glycolytic phenotype[10]. Finally, cancer-associated fibroblast-derived EVs induce central carbon metabolism in target cells and promote tumor growth under nutrient-deprivation or nutrient-stress conditions[11]. It has been recently hypothesized that EVs are involved in the intercellular trafficking of small molecules[11]. However, whether EVs can act as independent, metabolically active units, capable of perturbing the extracellular milieu, is still unknown. In this work, we sought to investigate the enzymatic activities associated with NSC-derived EVs. We found that NSC EVs are metabolically active and, in particular, that they exhibit L-asparaginase activity. We identified Asrgl1 as the key metabolic enzyme responsible for the L-asparaginase activity of EVs. Finally, we observed that EV-associated Asrgl1 is specific for asparagine (Asn) and is devoid of glutaminase activity. For the first time, to our knowledge, our study shows that EVs can behave as autonomous metabolic reactors and are capable of delivering specific and functional L-asparaginase activity to the microenvironment via Asrgl1.

RESULTS

NSCs secrete EVs containing exosomes

We started our investigation by generating EVs from NSCs. Stably expandable NSCs were derived from the subventricular zone of adult mice, and EVs were purified from NSC supernatants by differential centrifugation (**Supplementary Results**, **Supplementary Fig. 1a**) as described[6]. To characterize the population of vesicles secreted by NSCs, we applied a combination of nanoparticle tracking analysis (NTA), tunable resistive pulse sensing (TRPS) technology and western blot (WB) analysis. NTA identified a major peak

[1]Wellcome Trust–Medical Research Council Stem Cell Institute, Department of Clinical Neurosciences–Division of Stem Cell Neurobiology, and NIHR Biomedical Research Centre, University of Cambridge, Cambridge, UK. [2]MRC Cancer Unit, University of Cambridge, Hutchison/MRC Research Centre, Cambridge Biomedical Campus, Cambridge, UK. [3]European Molecular Biology Laboratory, European Bioinformatics Institute (EMBL-EBI), Wellcome Trust Genome Campus, Hinxton, Cambridge, UK. [4]Stroke Branch, National Institute of Neurological Disorders and Stroke, National Institutes of Health (NINDS/NIH), Bethesda, Maryland, USA. [5]Stem Cells Laboratory, Cell Factory and Biobank, Azienda Ospedaliera 'Santa Maria', Terni, Italy. [6]IRCCS Casa Sollievo della Sofferenza, Foggia, Italy. [7]Department of Biotechnology and Biosciences, University of Milano-Bicocca, Milano, Italy. [8]Medical Research Council–Elsie Widdowson Laboratory, Cambridge, UK. [9]Department of Engineering, Electrical Engineering Division, University of Cambridge, Cambridge, UK. [10]Present address: Department of Biomedical and Biotechnological Sciences (BIOMETEC), University of Catania, Catania, Italy. [11]These authors contributed equally to this work. *e-mail: cf366@MRC-CU.cam.ac.uk or spp24@cam.ac.uk
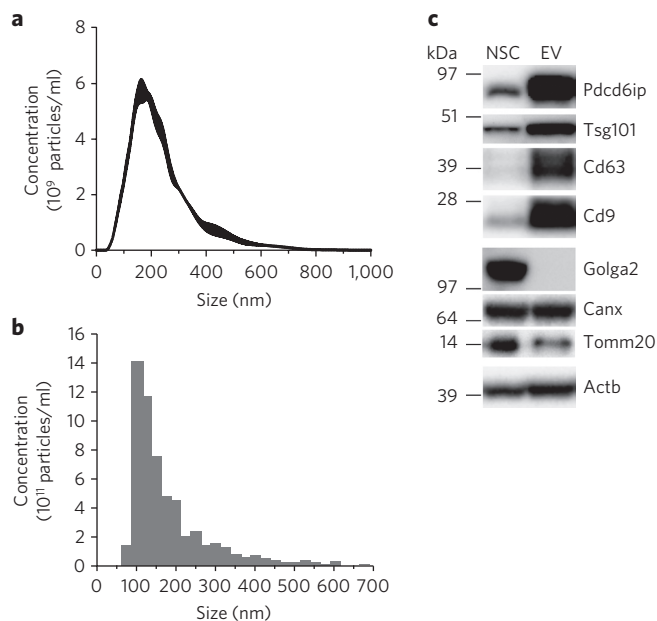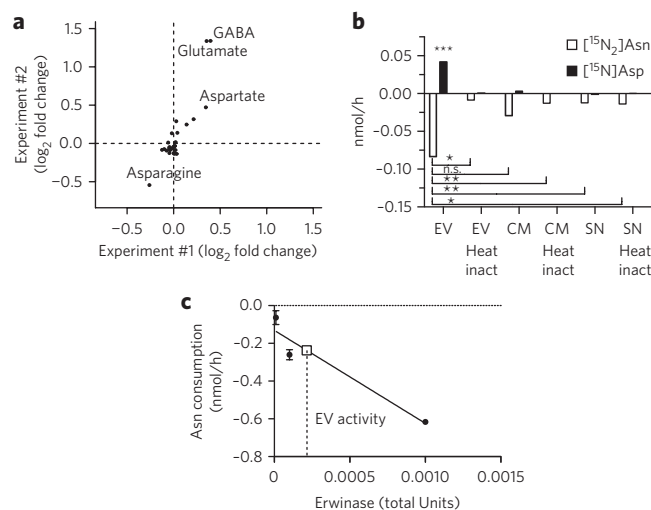
Figure 1 | NSCs secrete EVs containing exosomes. (**a**,**b**) Particle-size distribution of EVs by NTA (**a**) and TRPS (**b**) technologies. The dimension data are expressed as mean values ± s.e.m. from *n* = 3 independent experiments. (**c**) Western blot analysis of markers for exosomes and for different organelles (Golgi, endoplasmic reticulum and mitochondria) in mouse NSCs and EVs. Data in **c** is representative of *n* = 3 independent protein preparations showing the same trends. Full gels are located in **Supplementary Figure 7**.


Figure 2 | NSC EVs are metabolically active *in vitro*. (**a**) Scatter plot of metabolomics experiment showing $\log_2$ fold changes of extracellular metabolites in medium + EVs compared to medium only. Positive and negative values indicate production and consumption of metabolites, respectively. Data from two independent experiments are shown. (**b**) Barplot of the consumption of $[^{15}N_2]$Asn and production of $[^{15}N]$ Asp mediated by EVs, conditioned medium (CM, medium with EVs) and supernatant (SN, medium deprived of EVs), with or without heat inactivation (inact; 100 °C for 10 min). Data are mean ± s.e.m. and have been obtained from *n* = 2 independent experiments. Statistical analysis was performed using one-way ANOVA, followed by Bonferroni's test correction. *$P < 0.05$; **$P < 0.01$; ***$P < 0.001$; n.s., not significant. (**c**) Consumption of Asn with different amounts of clinical-grade L-asparaginase produced by *Erwinia chrysanthemi* (Erwinase) was used to determine the L-asparaginase activity associated with EVs. One International Unit of L-asparaginase is defined as the amount of enzyme required to generate 1 μmol of ammonia/min at pH 7.3 and 37 °C. Solid line indicates Erwinase calibration curve, and square symbol and dashed line indicate interpolation of the calibration curve with Asn consumption values obtained with EVs. Data are mean ± s.d. from one experiment.

(169 ± 3 nm) in the size range of exosomes, as well as a minor peak (300–500 nm), consistent with the dimensions of larger shedding vesicles (**Fig. 1a**). TRPS with a 150-nm nanopore confirmed the presence of small vesicles, showing a major peak corresponding to the size described for exosomes (102 ± 9 nm) (**Fig. 1b**)[12]. WB analyses further confirmed that protein extracts purified from EVs are specifically enriched in markers associated with exosomes (in comparison to parental NSC protein extracts), which include Pdcd6ip, Tsg101 and the tetraspanins CD63 and CD9. On the other hand, markers for other cellular compartments, such as Golga2 (Golgi), Calnexin (endoplasmic reticulum) and Tomm20 (mitochondria), did not show a similar distribution (**Fig. 1c**).

NSC EVs exhibit L-asparaginase activity

To assess the metabolic activity of NSC EVs, we incubated EVs in commercial NSC medium and analyzed the consumption and release of metabolites from, and in the medium via LC–MS (**Supplementary Fig. 1b**). We observed that incubation with EVs induced profound changes in the levels of several metabolites within the medium (**Supplementary Table 1**). Importantly, heat inactivation suppressed this metabolic activity of EVs (**Supplementary Fig. 2a**), suggesting that consumption and release of metabolites is largely due to the intrinsic enzymatic activity of EVs and not the leakage of metabolites. We found that Asn was the most consumed metabolite out of two independent EVs preparations, whereas aspartate (Asp) and glutamate (Glu) were among the most abundantly released metabolites (**Fig. 2a**). Given the substantial depletion of Asn coupled with the production of Asp, we hypothesized that EVs harbor L-asparaginase activity. To validate this hypothesis, we incubated EVs in commercial NSC medium supplemented with $[^{15}N_2]$ Asn. If EVs carried L-asparaginase activity, $[^{15}N]$Asp should be found in the spent EV medium (**Supplementary Fig. 2b**). Consistent with this hypothesis, we observed marked consumption of $[^{15}N_2]$Asn

coupled with production of $[^{15}N]$Asp in medium containing EVs (**Fig. 2b**). Notably, EVs exhibited enriched L-asparaginase activity compared to NSC conditioned media (CM) and EV-deprived NSC supernatants (SN). Furthermore, L-asparaginase activity was dampened in heat-inactivated EVs (**Fig. 2b**), confirming that this activity depends on intact enzymatic function. Importantly, we found that NSCs also exhibited L-asparaginase activity, as indicated by the uptake of Asn and intracellular conversion of $[^{15}N_2]$Asn to $[^{15}N]$Asp (**Supplementary Fig. 2c**). Finally, a calibration curve using clinical-grade L-asparaginase produced by *Erwinia chrysanthemi* (Erwinase) allowed us to quantify the intrinsic L-asparaginase activity of NSC EVs, giving a value of 2×10^{-6} U/μg of EV protein (**Fig. 2c**).

Mouse and human NSCs traffic Asrgl1 into EVs

We then investigated the identity of the possible enzymes that might confer such asparaginase activity to NSC-derived EVs. The mouse genome contains two L-asparaginases: a 60-kDa lysophospholipase/ L-asparaginase (Aspg; A0JNU3) and an isoaspartyl peptidase/ L-asparaginase (Asrgl1; Q8C0M9). To assess the expression of *Aspg* and *Asrgl1* in NSCs, we took advantage of a comprehensive long RNA-seq analysis that we recently published[6], and found that NSCs express *Asrgl1* but not *Aspg* (**Supplementary Fig. 3a**).

Independent qPCR and WB analyses confirmed the RNA-seq data, and showed that EV protein extracts contained Asrgl1 at levels comparable to those of parental NSCs (**Fig. 3a,b**). We then assessed
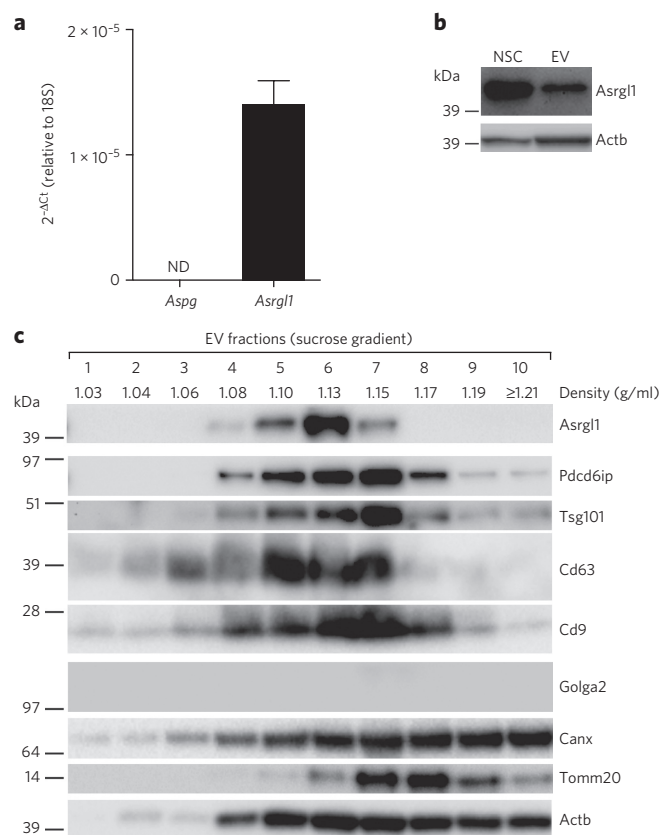
Figure 3 | Mouse NSCs traffic Asrgl1 into EVs. (**a,b**) qPCR (**a**) and western blot (**b**) analyses of Asrgl1 expression in mouse NSCs. qPCR data are represented as fold change ± s.e.m. of the *Aspg* and *Asrgl1* mRNA levels in NSCs, and analyzed with the $2^{-\Delta Ct}$ method over *18S* ribosomal RNA, used as housekeeping gene. Both qPCR and WB data have been obtained from *n* = 3 independent experiments. Actb, sample processing control; ND, not determined. (**c**) Western blot of Asrgl1 and markers for exosomes and cellular organelles, as in **Figure 1**, after sucrose gradient fractionation of total EVs. Data in **c** is representative of *n* = 3 independent protein preparations showing the same trends. See also **Supplementary Figure 3**. Full gels are located in **Supplementary Figures 8–10**.
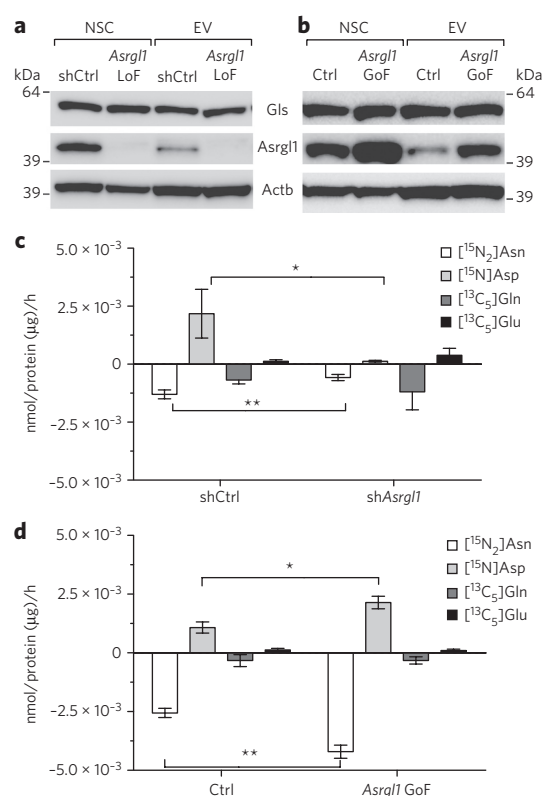

Figure 4 | Asrgl1 is responsible for the selective L-asparaginase activity associated with EVs. (**a,b**) Western blot analysis of sh*Asrgl1* Lof (**a**) and *Asrgl1* GoF (**b**) NSCs and EVs. Data are representative of *n* = 3 independent protein preparations showing the same trends. shCtrl, non-target shRNA control; Ctrl, empty vector. (**c,d**) Barplot of the consumption of [$^{15}N_2$]Asn and [$^{13}C_5$]Gln followed by production of [^{15}N]Asp and [$^{13}C_5$]Glu mediated by sh*Asrgl1* (**c**) and *Asrgl1* GoF (**d**) EVs. Data are mean ± s.e.m. and have been obtained from *n* ≥ 3 independent experiments. Statistical analysis was performed using two-sided *t*-test. *$P < 0.05$; **$P < 0.01$. Full gels are located in **Supplementary Figures 11** and **12**.

the distribution of the enzyme in EVs subjected to sucrose gradient fractionation. We found that Asrgl1 peaks at 1.13 g/ml, overlapping with the exosome fraction, both in terms of markers (i.e., Pdcd6ip, Tsg101, CD63 and CD9) and of density (1.13–1.20 g/ml), as previously described[13] (**Fig. 3c**). We also excluded the possibility that Asrgl1 was present in fractions enriched into protein aggregates (density ≥1.21 g/ml)[14] (**Fig. 3c**), thus unambiguously demonstrating that Asrgl1 is genuinely associated with EVs (for example, shedding vesicles and exosomes).

Next, we extended our analyses to clinical-grade human fetal NSCs (hNSCs)[15], as well as to EVs collected from hNSC supernatants. Similar to the results observed in mouse NSCs, hNSCs expressed *ASRGL1*, but not *ASPG*, and hNSC-derived EVs contained *ASRGL1* (**Supplementary Fig. 3b,c**). Thus, EVs from both mouse and human NSCs are 'cargoed' with Asrgl1.

Asrgl1 catalyzes the L-asparaginase activity of EVs

Asrgl1 has been shown to be associated with small exosome-like vesicles called prostasomes[16], but its metabolic function in EVs remains to be defined.

In vitro experiments indicate that, unlike bacterial Aspg, Asrgl1 is devoid of enzymatic activity toward glutamine (Gln)[17]. Therefore, we

wanted to investigate substrate specificity of EV-associated Asrgl1. We first tested whether EVs exhibit any glutaminase (Gls) activity. To this aim, we incubated EVs with [^{13}C]Gln and measured the production of [^{13}C]Glu, the product of Gls activity (see **Supplementary Fig. 4a** for a schematic of the experiment). We could detect Gln consumption by EVs, which was associated with the production of [^{13}C]Glu (**Supplementary Fig. 4b**). Heat inactivation abolished Gln consumption and Glu production by EVs, indicating that this activity requires the presence of intact enzymes. In line with this finding, we detected protein expression of Gls in EVs (**Fig. 4a,b**).

To confirm that Asrgl1 is the L-asparaginase responsible for the EV-mediated hydrolysis of Asn to Asp, and further exclude any possible Asrgl1-related Gls activity, we performed loss- and gain-of-function (LoF and GoF, respectively) experiments by transducing NSCs with either a short-hairpin RNA targeting *Asrgl1* (sh*Asrgl1*) or with the *Asrgl1* coding sequence. NSC transduction with LoF and GoF lentiviral vectors did not affect NSC growth and viability upon serial passaging *in vitro* (**Supplementary Fig. 5**). LoF and GoF NSCs and EVs showed effective reductions and increases in the levels of Asrgl1 expression, respectively, as compared to non-target shRNA control (shCtrl) and empty vector (Ctrl), respectively. Of note, these changes in the expression of Asrgl1 had no effects on the levels of other endogenous enzymes, such as Gls, both in NSC and EVs (**Fig. 4a,b**).

We then assessed the relative metabolic activity of EV-trafficked Asrgl1 by incubating control, LoF and GoF EVs in cell culture medium containing equal amounts of Asn and Gln. Consumption of [^{15}N$_2$]Asn and production of [^{15}N]Asp were significantly reduced in medium incubated with sh*Asrgl1* EVs (compared to those with shCtrl EVs) (**Fig. 4c**). Conversely, we observed a significant increase in the consumption of [^{15}N$_2$]Asn and production of [^{15}N]Asp within medium incubated with *Asrgl1* GoF EVs (compared to those with Ctrl EVs) (**Fig. 4d**). Importantly, incubation of medium with both sh*Asrgl1* EVs and *Asrgl1* GoF EVs did not alter the consumption of [^{13}C$_5$]Gln or the production of [^{13}C$_5$]Glu (**Fig. 4c,d**), confirming that Asrgl1 activity is specific for Asn and is devoid of Gls activity. Finally, we compared the L-asparaginase activity of EVs to that of parental cells and of human recombinant ASRGL1 in solution as resuspended protein. We used the latter as reference to estimate by western blotting the relative abundance of Asrgl1 in NSCs and EVs, both Ctrl and GoF. Interestingly, we found that NSCs and EVs both exhibit much higher Asrgl1-dependent L-asparaginase activity compared to the recombinant protein (**Supplementary Fig. 6**).

DISCUSSION

EVs are influential players in intercellular communication, participating via exchanging lipids, proteins and nucleic acids. Depending on their origin and cargo molecules, EVs can modulate immunoregulatory processes, set up tumor escape mechanisms and/or mediate regenerative or degenerative processes[18]. The extent to which EVs interact with and modulate intracellular signaling pathways within target cells is not yet fully understood[19].

We have recently shown that NSC EVs carrying receptor proteins within their cargo, including inflammatory cytokine receptors, activate downstream canonical signaling pathways in target cells, a mechanism that grafted stem cells might use to communicate with the host immune system[6]. More complex mechanisms, however, are emerging, including direct gene and/or protein delivery or transfer of noncoding small RNAs (for example, microRNAs) functioning in RNA silencing and post-transcriptional regulation of gene expression[20]. The level of complexity in the understanding of signaling properties of EVs increases along with the knowledge that (i) individual cells release different subtypes of EVs simultaneously, and intercellular communication often involves more than two cells; (ii) trafficking of messengers into EVs varies in response to perturbations and stresses, including cytokines and growth factors, relative levels of extra- or intracellular amino acids[21], hypoxia and normoxia, shear stress and circadian rhythms[22,23] and (iii) available techniques to collect, process and analyze EVs and EV-induced cellular responses remain suboptimal[24].

Emerging evidence suggests that EVs from different cell types can act as metabolic regulators[7–11], yet the characterization of EVs intrinsic metabolic activity is still being debated. By applying state-of-the-art untargeted and targeted metabolomic analyses, we demonstrated that NSC EVs exhibit enzymatic activities that affect the consumption and release of metabolites in the extracellular compartment. This important observation suggests that EVs are metabolically active and that multiple enzymes are associated with EVs. Unexpectedly, we found that Asn is the most substantially consumed metabolite, suggesting a predominant L-asparaginase activity associated with EVs. Notably, this L-asparaginase activity was observed in NSCs, strongly suggesting that EVs do not acquire this metabolic function *de novo*, but, rather, this activity is transferred from the donor cells. This hypothesis has important implications: whereas L-asparaginase activity in NSCs would result in a possible depletion of Asn in the extracellular milieu, L-asparaginase activity in EVs has the additional benefit of releasing Asp, a metabolite whose role in supporting cells' bioenergetics is increasingly recognized[25,26]. Hence, the biological consequences of Asn-depletion strategies using NSCs or EVs are likely to be very different.

Aside from Asn, the levels of several other metabolites with known biological functions were substantially altered by EVs. These include Asp, Glu, lactate, GABA and alanine. For instance, GABA and Glu are well-known neurotransmitters that are able to shape the activity of brain cells[27] as well as the behavior of other cell types[28,29]. Lactate is a potent signaling molecule able to affect the proliferation of cancer cells[30], promote tumor angiogenesis[31] and act as a pro-inflammatory signal to induce T cell migration[32]. Finally, uptake of Asp has recently been shown to be essential for cells with impaired mitochondrial function both *in vitro* and *in vivo*[25,26]. This evidence supports the hypothesis that, by altering the metabolic composition of the microenvironment, EVs might be able to profoundly shape the behavior of surrounding cells, with important potential implications for biological functions of different cell types.

Here we identified Asrgl1 as the key metabolic enzyme responsible for the EV-associated L-asparaginase activity. Asrgl1 was initially identified as novel L-asparaginase in the rat and human testis[33], and has lately been found to exhibit specific activity for Asn[17]. We demonstrated that Asrgl1 is the only metabolic enzyme with known L-asparaginase activity expressed by mouse and human NSCs, which both export toward EVs. Moreover, when equimolar amounts of labeled Asn and Gln are added to medium, the relative L-asparaginase activity is higher compared to the Gls activity, further supporting that the L-asparaginase activity is predominant in EVs. We also confirmed that Asrgl1 is the enzyme responsible for the Asn-specific L-asparaginase activity mediated by EVs, as indicated by our Asrgl1 Lof and GoF experiments. In fact, when the expression of Asrgl1 was reduced or enhanced, we observed that, while Gln and Glu levels were unaltered, only Asn consumption and Asp production were affected.

The finding that EV-derived Asrgl1 is specific for Asn has important clinical implications. Various bacteria-derived L-asparaginases are currently used to treat acute lymphoblastic leukemia and malignant lymphoma[34]. Furthermore, new reports demonstrated L-asparaginase efficacy also toward glioblastoma cells *in vitro*[35]. The residual Gls activity of bacterial asparaginases is thought to be a major drawback of therapy, as it leads to secondary immune depression and liver toxicity[36]. Therefore, the identification of Gls-free functional L-asparaginase in EVs might provide a valid alternative to recombinant L-asparaginases that would limit most of their side effects.

Beyond the characterization of EV-associated Asrgl1 activity, the mechanism of Asrgl1 action within the EV compartment remains to be further elucidated. Considering its cytosolic localization, it is tempting to speculate that Asrgl1 may be contained in the lumen of EVs, where it would remain functionally active for at least 24 h, a time frame that is compatible with the experiments described here. Indeed, Asrgl1 enzymatic activity is significantly enriched in EVs as compared to EV-deprived NSC supernatants, which indicates that extracellular metabolic enzymes are not secreted as free proteins in the extracellular milieu. Furthermore, the observation that the intrinsic Asrgl1 activity is higher in EVs than in NSCs and in the recombinant protein suggests that Asrgl1 in EVs might be exposed to an activating microenvironment or subject to post-translational modifications that do not occur *in vitro*, making EVs ideal vessels to deliver this enzyme.

Applying heavy–light double stable isotope labeling of amino acids in cell culture (SILAC) comparing EVs and exosomes collected from NSCs, we have recently shown that NSCs and NSC EVs express a few members of the solute carrier (SLC) family of membrane transporters, which include the high-affinity Glu and Asp transporter (Slc1a3), the two-system A family members the sodium-coupled neutral amino acid transporter 2 (Slc38a2) and the sodium-coupled neutral amino acid transporter 3 (Slc38a3)[6]. It would then be plausible to hypothesize that metabolically active EVs uptake extracellular Asn via sodium-coupled neutral amino

acid (system N/A) transporters (SNATs), hydrolyze Asn to Asp into Asrgl1-cargoed EVs and then export Asp via EV-associated Slc1a3 in the extracellular milieu. Further studies are necessary to validate this hypothesis, as well as to identify the possible mechanisms by which metabolic enzymes are loaded into (or sampled by) EVs.

In conclusion, our work shows, for the first time, the intrinsic ability of NSCs to deliver functional L-asparaginase activity in the microenvironment via Asrgl1 in EVs. Our work further highlights a surprising new role for stem-cell-derived EVs, with a potential role in the propagation of specific metabolic signals to the surrounding cells and to the microenvironment.

METHODS
Methods, including statements of data availability and any associated accession codes and references, are available in the online version of the paper.

References
1. Deatherage, B.L. & Cookson, B.T. Membrane vesicle release in bacteria, eukaryotes, and archaea: a conserved yet underappreciated aspect of microbial life. *Infect. Immun.* **80**, 1948–1957 (2012).
2. Raposo, G. & Stoorvogel, W. Extracellular vesicles: exosomes, microvesicles, and friends. *J. Cell Biol.* **200**, 373–383 (2013).
3. Kim, D.K., Lee, J., Simpson, R.J., Lötvall, J. & Gho, Y.S. EVpedia: A community web resource for prokaryotic and eukaryotic extracellular vesicles research. *Semin. Cell Dev. Biol.* **40**, 4–7 (2015).
4. Kalra, H. *et al.* Vesiclepedia: a compendium for extracellular vesicles with continuous community annotation. *PLoS Biol.* **10**, e1001450 (2012).
5. Théry, C., Ostrowski, M. & Segura, E. Membrane vesicles as conveyors of immune responses. *Nat. Rev. Immunol.* **9**, 581–593 (2009).
6. Cossetti, C. *et al.* Extracellular vesicles from neural stem cells transfer IFN-γ via Ifngr1 to activate Stat1 signaling in target cells. *Mol. Cell* **56**, 193–204 (2014).
7. Garcia, N.A., Moncayo-Arlandi, J., Sepulveda, P. & Diez-Juan, A. Cardiomyocyte exosomes regulate glycolytic flux in endothelium by direct transfer of GLUT transporters and glycolytic enzymes. *Cardiovasc. Res.* **109**, 397–408 (2016).
8. Ronquist, K.G., Ek, B., Stavreus-Evers, A., Larsson, A. & Ronquist, G. Human prostasomes express glycolytic enzymes with capacity for ATP production. *Am. J. Physiol. Endocrinol. Metab.* **304**, E576–E582 (2013).
9. Minciacchi, V.R. *et al.* Large oncosomes contain distinct protein cargo and represent a separate functional class of tumor-derived extracellular vesicles. *Oncotarget* **6**, 11327–11341 (2015).
10. Johnson, S.M. *et al.* Metabolic reprogramming of bone marrow stromal cells by leukemic extracellular vesicles in acute lymphoblastic leukemia. *Blood* **128**, 453–456 (2016).
11. Zhao, H. *et al.* Tumor microenvironment derived exosomes pleiotropically modulate cancer cell metabolism. *eLife* **5**, e10250 (2016).
12. Lobb, R.J. *et al.* Optimized exosome isolation protocol for cell culture supernatant and human plasma. *J. Extracell. Vesicles* **4**, 27031 (2015).
13. Théry, C. *et al.* Molecular characterization of dendritic cell-derived exosomes. Selective accumulation of the heat shock protein hsc73. *J. Cell Biol.* **147**, 599–610 (1999).
14. Quillin, M.L. & Matthews, B.W. Accurate calculation of the density of proteins. *Acta Crystallogr. D Biol. Crystallogr.* **56**, 791–794 (2000).
15. Mazzini, L. *et al.* Human neural stem cell transplantation in ALS: initial results from a phase I trial. *J. Transl. Med.* **13**, 17 (2015).
16. Poliakov, A., Spilman, M., Dokland, T., Amling, C.L. & Mobley, J.A. Structural heterogeneity and protein composition of exosome-like vesicles (prostasomes) in human semen. *Prostate* **69**, 159–167 (2009).
17. Cantor, J.R., Stone, E.M., Chantranupong, L. & Georgiou, G. The human asparaginase-like protein 1 hASRGL1 is an Ntn hydrolase with β-aspartyl peptidase activity. *Biochemistry* **48**, 11026–11031 (2009).
18. Kourembanas, S. Exosomes: vehicles of intercellular signaling, biomarkers, and vectors of cell therapy. *Annu. Rev. Physiol.* **77**, 13–27 (2015).
19. Tkach, M. & Théry, C. Communication by extracellular vesicles: where we are and where we need to go. *Cell* **164**, 1226–1232 (2016).
20. Xu, L., Yang, B.F. & Ai, J. MicroRNA transport: a new way in cell communication. *J. Cell. Physiol.* **228**, 1713–1719 (2013).
21. Fafournoux, P., Bruhat, A. & Jousse, C. Amino acid regulation of gene expression. *Biochem. J.* **351**, 1–12 (2000).
22. Braicu, C. *et al.* Exosomes as divine messengers: are they the Hermes of modern molecular oncology? *Cell Death Differ.* **22**, 34–45 (2015).
23. Christie, G.R., Hyde, R. & Hundal, H.S. Regulation of amino acid transporters by amino acid availability. *Curr. Opin. Clin. Nutr. Metab. Care* **4**, 425–431 (2001).
24. Witwer, K.W. *et al.* Standardization of sample collection, isolation and analysis methods in extracellular vesicle research. *J. Extracell. Vesicles* **2**, (2013).
25. Birsoy, K. *et al.* An essential role of the mitochondrial electron transport chain in cell proliferation is to enable aspartate synthesis. *Cell* **162**, 540–551 (2015).
26. Sullivan, L.B. *et al.* Supporting aspartate biosynthesis is an essential function of respiration in proliferating cells. *Cell* **162**, 552–563 (2015).
27. Petroff, O.A. GABA and glutamate in the human brain. *Neuroscientist* **8**, 562–573 (2002).
28. Watanabe, M. *et al.* Gamma-aminobutyric acid (GABA) and cell proliferation: focus on cancer cells. *Histol. Histopathol.* **21**, 1135–1141 (2006).
29. Stepulak, A., Rola, R., Polberg, K. & Ikonomidou, C. Glutamate and its receptors in cancer. *J. Neural Transm. (Vienna)* **121**, 933–944 (2014).
30. Pavlides, S. *et al.* The reverse Warburg effect: aerobic glycolysis in cancer associated fibroblasts and the tumor stroma. *Cell Cycle* **8**, 3984–4001 (2009).
31. Sonveaux, P. *et al.* Targeting the lactate transporter MCT1 in endothelial cells inhibits lactate-induced HIF-1 activation and tumor angiogenesis. *PLoS One* **7**, e33418 (2012).
32. Haas, R. *et al.* Lactate regulates metabolic and pro-inflammatory circuits in control of T cell migration and effector functions. *PLoS Biol.* **13**, e1002202 (2015).
33. Bush, L.A. *et al.* A novel asparaginase-like protein is a sperm autoantigen in rats. *Mol. Reprod. Dev.* **62**, 233–247 (2002).
34. Duval, M. *et al.* Comparison of *Escherichia coli*-asparaginase with Erwinia-asparaginase in the treatment of childhood lymphoid malignancies: results of a randomized European Organisation for Research and Treatment of Cancer-Children's Leukemia Group phase 3 trial. *Blood* **99**, 2734–2739 (2002).
35. Karpel-Massler, G. *et al.* Metabolic reprogramming of glioblastoma cells by L-asparaginase sensitizes for apoptosis *in vitro* and *in vivo*. *Oncotarget* **7**, 33512–33528 (2016).
36. Ollenschläger, G. *et al.* Asparaginase-induced derangements of glutamine metabolism: the pathogenetic basis for some drug-related side-effects. *Eur. J. Clin. Invest.* **18**, 512–516 (1988).

Author contributions
N.I., E.G., C.F. and S.P. conceived the study and designed the experiments; N.I., T.L., C.C., L.P.-J., J.D.B. and M.G. elucidated the trafficking of Asrgl1 into NSC EVs, and performed experiments including cell culture preparations, EV purification from media, tunable sensitive pulse sensing, western blots, RT and qPCR, vector production and generation of gain-of-function and loss-of-function tools; N.I., C.B. and N.F. performed nanoparticle tracking analysis; A.S.H.C. and E.G. performed the LC–MS metabolomic analyses; A.L.V., L.G.O., C.F. and S.P. provided key reagents and resources; N.I., E.G., A.S.H.C., T.L., H.K.S., A.J.E., C.F. and S.P. analyzed the data and interpreted and discussed the results; N.I., E.G., C.F. and S.P. prepared the figures and wrote and edited the manuscript; C.F. and S.P. supervised the research.

Competing financial interests
The authors declare competing financial interests: details accompany the online version of the paper.

Additional information
Any supplementary information, chemical compound information and source data are available in the online version of the paper. Reprints and permissions information is available online at http://www.nature.com/reprints/index.html. Publisher's note: Springer Nature remains neutral with regard to jurisdictional claims in published maps and institutional affiliations. Correspondence and requests for materials should be addressed to C.F. or S.P.

ONLINE METHODS

Cell culture preparations. NSCs were prepared from the subventricular zone of 7- to 12-week-old SJL mice, as described[1]. Good Manufacturing Practice–grade, fetal human NSCs from natural *in utero* death (hNSCs) were prepared as described[15]. Both mouse and human NSCs were tested for mycoplasma contamination, several times throughout the study, and the results were always mycoplasma free.

Purification of EVs from media and sucrose gradient fractionation. Mouse and human NSC EVs were collected and characterized as described[5].

Nanoparticle tracking analysis (NTA). Samples were diluted 1:1,000 with PBS, vortexed and analyzed by NTA instrument (NS500, NanoSight ltd) fitted with an Electron Multiplication Charge-Couple Device camera and a 532-nm laser. The temperature was maintained within the range of 20–25 °C and resultant liquid viscosity calculated by the instrument. Three repeated measurements of 60 s were recorded for each of the three independent samples (nine analyses in total). Fresh sample was loaded into the chamber before each video capture. Static mode (no flow) was used for analysis and detection threshold was adjusted to 5. Automatic settings were set for blur size, minimum track length and minimum particle size. The movement of each particle in the field of view was measured to generate the average displacement (in terms of x and y) of each particle per unit time. From this measurement, the particle diffusion coefficient was estimated and the hydrodynamic diameter calculated through application of the Stokes-Einstein equation.

Tunable resistive pulse sensing (TRPS). The concentration and size distribution of EVs was analyzed with TRPS (qNano, Izon Science Ltd.) using a NP150 nanopore at 0.5 V with 47 mm stretch. The concentration of particles was standardized using 100 nm calibration beads (CPC 100) at a concentration of 1×10^{10} particles/ml.

Protein purification and western blot analysis. Whole NSCs, EVs and sucrose gradient fraction extracts were processed as described[5]. Due to the limited amount of material obtained from sucrose gradient fractions, the correspondent WBs were performed using independent EV preparations starting from the same NSC batch. The following primary antibodies were used: mouse monoclonal anti-Pdcd6ip (BD Transduction Lab catalog no. 611620); rat monoclonal and mouse monoclonal anti-CD9 (BD Transduction Lab catalog no. 553758 and Life Technologies catalog no. 10626D, respectively); goat polyclonal anti-TSG101 (Santa Cruz catalog no. sc-6037); rat monoclonal and mouse monoclonal anti-CD63 (MBL catalog no. D263-3 and Life Technologies catalog no. 10628D, respectively); rabbit polyclonal anti-Asrgl1 (Proteintech catalog no. 11400-1-AP); mouse monoclonal anti-GM-130 (BD Transduction Lab catalog no. 610823); rabbit polyclonal anti-calnexin (Abcam catalog no. ab22595); rabbit polyclonal anti-Tom-20 (Santa Cruz catalog no. sc-11415); rabbit monoclonal anti-Gls (Abcam catalog no. ab156876); mouse monoclonal anti-beta-Actin (Sigma catalog no. A1978). Molecular weight marker: SeeBlue Plus2 (Invitrogen). WB for mouse and human Cd63 and Cd9 were run under nonreducing conditions, i.e., sample buffer used for electrophoresis was devoid of reducing agent.

RNA extraction, RT and qPCR. RNAs from mouse and human NSCs were obtained using the miRCURY RNA Isolation Kit – Cell & Plant (Exiqon). Total RNA quantity and purity were assessed with the NanoDrop 2000c instrument (Thermo Scientific). cDNA synthesis was performed using SuperScript III First-Strand Synthesis SuperMix for qRT-PCR (Invitrogen), with random hexamers as primers. qPCR was performed with the TaqMan Universal PCR Master Mix (Applied Biosystems) and TaqMan Gene Expression Assays for FAM *Aspg*, *Asrgl1*, *ASPG* and *ASRGL1* and VIC euk *18S* rRNA probes. Samples were tested in triplicate on a QuantStudio 7 Flex Real-Time PCR System (Applied Biosystems) and analyzed with the $2^{-\Delta Ct}$ method over 18S ribosomal RNA, used as housekeeping gene.

Vector production, titration and NSC infection. Lentiviral particles were obtained and used as described[37]. sh*Asrgl1* NSCs (*Asrgl1* LoF) were obtained using the pLKO.1-puro third generation vector (Sigma) with the shRNA sequence TRCN32311 (CCGGCCAGAGTTCAACGCAGGT TATCTCGAGATAACCTGCGTTGAACTCTGGTTTTTG) targeting mouse Asrgl1. *Asrgl1* GoF NSCs were obtained using the pCDH-EF1-MCS-T2A-GFP third generation vector (System Biosciences) with the coding sequence expressing the mouse Asrgl1. A multiplicity of infection (MOI) of 30 was used for both sh*Asrgl1* and *Asrgl1* GoF NSCs.

LC–MS metabolomic analysis. For the LC separation, column used was the SeQuant ZIC-HILIC (150 mm × 4.6 mm, particle size 5 µm) with a guard column (20 mm × 2.1 mm, 5 µm) from Merck Millipore (HiChrom, Reading, UK). Mobile phase A: 0.1% formic acid v/v in water. Mobile B: 0.1% formic acid v/v in acetonitrile. The flow rate was kept at 300 µl/min and gradient was as follows: 0 min 80% of B, 12 min 50% of B, 26 min 50% of B, 28 min 20% of B, 36 min 20% of B, and 37–45 min 80% of B. The mass spectrometer (Thermo Q-Exactive Orbitrap) was operated in a polarity-switching mode. Samples were randomized to avoid bias due to machine drift. Chromatographic peaks were integrated using XCalibur Quan software (Thermo).

Untargeted metabolomics and metabolic tracing analyses. DMEM high glucose (Life Technology) was incubated for 24 h at 37 °C and 5% CO_2 with or without isolated EVs, corresponding to 100 µg of protein extract. To compare metabolic activities of EVs, conditioned medium (CM) and supernatant (SN), medium was supplemented with 50 µM L-$[^{15}N_2]$Asn and 2.5 mM $[^{13}C_5]$Gln and incubated for 24 h at 37 °C and 5% CO_2 with or without isolated EVs. For all other isotope tracing experiments, medium was supplemented with equimolar concentrations of L-$[^{15}N_2]$Asn and $[^{13}C_5]$Gln (50 µM). To assess NSC L-asparaginase activity 1.5×10^6 Ctrl or Asrgl1 GoF cells were seeded in 6-well plates and incubated at 37 °C with medium containing 50 µM L-$[^{15}N_2]$Asn for 24 h. At the end of the incubation period, cells or EVs were harvested and centrifuged for 5 min at 300g or 30 min at 100,000g, respectively. Supernatants were collected and NPC pellets were washed three times in PBS. Extracellular metabolites were extracted by diluting 50 µl of supernatant in 750 µl extraction buffer (EB; MeOH:ACCN:H_2O, 50:30:20). NSC intracellular metabolites were extracted by resuspending washed cellular pellets in EB (1 ml/10^6 cells). Extracted samples were mixed at 4 °C for 15 min and proteins were precipitated by centrifugation at 16,000g at 4 °C for 10 min. Supernatant was collected and submitted to LC–MS analysis. To investigate extracellular metabolic activity, LC–MS peak areas of fresh medium were compared to EVs spent medium. Absolute quantification of metabolites was obtained by comparing external standard curves composed of at least 4 dilution points.

Quantification of Asrgl1 activity in intact NSCs and EVs was performed by quantifying Asrgl1 protein abundance in the different fractions. ImageJ was used to quantify the signal of the active form (alpha-chain) of *ASRGL1* and to extrapolate the amount of Asrgl1 in NSCs and EVs. $[^{15}N]$Asn consumption from NSCs, EVs, and recombinant protein was measured using LC–MS and normalized to Asrgl1 content.

Statistical analysis. For untargeted metabolomics analysis, statistical analysis was performed with the R package "muma" (https://cran.r-project.org/) by comparing levels of metabolites in fresh and EVs conditioned medium via student's t-test. Benjamini–Hochberg correction for multiple testing and false discovery rate (FDR) = 0.05 were applied to determine statistical significance. For isotope tracing experiments statistical analysis was performed with Prism Graphpad and tests were applied as indicated in figure legends.

Data availability. Requests for materials, associated protocols, and other supporting data should be sent to the corresponding authors.

37. Iraci, N., Tyzack, G.E., Cossetti, C., Alfaro-Cervello, C. & Pluchino, S. Viral manipulation of neural stem/precursor cells. *Neuromethods* **82**, 269–288 (2013).